Int. J. Nano Dimens., 12 (4): 369-379, Autumn 2021

ORIGINAL ARTICLE

# A novel method for the fabrication of proton conducting and antimicrobial Tin Cerium Phosphate-polyaniline nanocomposite ion exchange material

***Vinisha Valsaraj Puthiyandi*, Janardanan Chathoth***

*Post-Graduate and Research Department of Chemistry, Sree Narayana College, Kannur-670 007, Kerala, India*

Received 02 March 2021, revised 17 May 2021, accepted 19 May 2021, available online 29 May 2021

**Abstract**

In-situ polymerization method was adapted to prepare a novel tin cerium phosphate-polyaniline nano composite ion exchange material. The physico-chemical properties of the material were determined using Fourier Transform Infra-Red (FTIR) Spectroscopy, Scanning Electron Microscopy (SEM), Thermogravimetric Analysis (TGA), and X-ray diffraction (XRD). X-ray diffraction study showed that the composite material formed is highly crystalline in nature, whereas its inorganic counterpart, tin cerium phosphate is amorphous in nature. The composite was formed in the nano range. SEM image of the composite depicts its needle-like morphology. The pH titration studies revealed bifunctional strong acid behavior of the exchanger. The newly synthesized composite materials exhibit better ion exchange capacity as well as better thermal and chemical stability than known materials. The material was found to be highly selective for toxic heavy metal ions like Pb(II) based on distribution studies,. The material also demonstrated good adsorbent capability for organic pollutants like dyes from an aqueous solution. The proton conducting behavior of the nano composite was studied using a solatron (1255B FRA FI1287 Electrochemical Phase) impedance analyzer and showed proton conductivity of the order of $10^{-3}$ S $cm^{-1}$. The antibacterial activity of tin cerium phosphate-polyaniline was explored against staphylococcus aureus. The results confirmed the bacteriostatic nature of the material.

**Keywords:** *Adsorption; Antibacterial Activity; Ion Exchange Capacity; Nano Composite; Polyaniline; Proton Conductivity.*

**How to cite this article**

*Valsaraj Puthiyandi V, Chathoth J. A novel method for the fabrication of proton conducting and antimicrobial Tin Cerium Phosphate-polyaniline nanocomposite ion exchange material. Int. J. Nano Dimens., 2021; 12(4): 369-379.*

## INTRODUCTION

During the past 15 years, the development of organic-inorganic hybrid materials has attracted much attention in a multitude of application arenas because of their intrinsically smart multifunctional character. The unusual and unique physicochemical and surface properties of these nanocomposite materials exploit their use in the high added-value applications such as coatings for corrosion protection and abrasion resistance, artificial membranes for ultra- and nano-filtration, adsorbents for toxic compounds and materials with specific optical, electrical, or magnetic properties for telecommunications or information displays [1-5]. The hybrid materials often show the best properties of each of their components in a synergic way by modifying their chemical, physical, and mechanical properties [6-9].

Composite materials comprising inorganic candidate materials into organic polymer matrices are gaining substantial attention from the research fraternity for its high performance, multi-functionality as exotic nanocomposite materials, ability to custom-design the architecture of the microstructure and thus their peculiar wide reaching application spectrum. A plethora of methods for preparing these hybrid materials have been reported [10–14]. The conversion of inorganic ion-exchangers into composite ion exchange materials is one of the latest developments in this exciting scientific discipline

* Corresponding Author Email: *vinipunep@gmail.com*

[15-17]. These materials are extensively used in the areas of chemical sensors, chromatography, fabrication of selective materials, and also have electrical and electronic applications. An inorganic precipitate ion-exchanger based on organic polymeric matrix is of great demands it possesses the required durable mechanical stability due to the presence of organic polymeric species and also exhibit the basic characteristics of an inorganic ion-exchanger with selectivity towards some particular metal ions [18-22]. We have synthesized such an interesting hybrid ion-exchanger that has a good ion-exchange capacity (IEC), high stability, reproducibility, and selectivity towards heavy metal ions for environmental applications especially those which helps in pollution abatement. For this purpose, we selected polyaniline, the aryl amine that has received great exposure since its rediscovery by Shirakawa [23]. All of the previously reported conducting polymer-based composite ion exchangers based on polyaniline were prepared by direct mixing of synthesized polyaniline with a matrix of inorganic ion exchangers [24, 25].

Some microbial organisms showed certain amount of resistance towards different antibiotics due to the continuous raise in the use of antibiotics. Considering this fact, researchers are forced to consider novel routes to arrive at effectively different antibiotics with enhanced microbial resistance. The nanomaterials based on metal ions showed wide range of biocidal activity against different harmful fungi, bacteria, and viruses [26]. Various researchers have considerable attention on antibacterial activities of nanocomposite ion exchange materials against pathogenic bacteria [27, 28]. As they are cost effective and at the same time possess low toxicity to human cells, they can be considered as better substitute to antibiotics. Their antibacterial effect takes place through its mechanism of binding and penetration through the bacterial cell wall. The literature survey revealed that no work has been known about the synthesis and antibacterial activity of tin cerium phosphate-polyaniline nanocomposite ion exchanger.

In this paper, we report the preparation of a composite of polyaniline conducting polymer and tin cerium phosphate inorganic ion exchanger by a combined process of simultaneous gelation of an inorganic acid salt, as well as polymerization of aniline monomer using in-situ polymerization techniques. We have characterized this material using various instrumental and non-instrumental techniques and conducted detailed qualitative and quantitative study on their ion exchange properties, dye adsorption capability, proton conductivity and antibacterial activity against *staphylococcus aureus* bacteria.

## MATERIALS AND METHODS

*Reagents:* Stannic chloride (E. Merck), ammonium ceric nitrate (E. Merck), sodium dihydrogen phosphate (Loba Chem), and aniline (E. Merck) were used for the synthesis of the exchangers. All other reagents and chemicals used were of analytical grade.

*Apparatus and instruments:* A glass column was used for column operations. An ELICO LI613 pH meter was used for pH measurements. Thermo-Nicolet Avtar 370 FT-IR Spectrometer was used for IR studies, Bruker AXS D8 Advance X-ray Diffractometer for x-ray diffraction studies, JEOL Model JSM - 6390LV for the scanning electron microscopic analysis, TG Perkin Elmer Diamond TG/DTA Analysis System for thermogravimetric/ derivative thermogravimetric analysis and JASCO V660 UV-visible spectrophotometer was used for spectrophotometric measurements.

*Synthesis of tin cerium phosphate-polyaniline (SnCeP-PANI):* Ammonium ceric nitrate solution (0.05 M), stannic chloride solution (0.05 M), and sodium dihydrogen phosphate solution (0.05 M) were prepared. Sodium dihydrogen phosphate solution was added to mixtures of ammonium ceric nitrate solution and stannic chloride solution with constant stirring in volume ratios of 1:2:3 corresponding to Sn : Ce : $PO_4$ and tin cerium phosphate gel was prepared. For synthesis of the composite, we added acidic solution of aniline monomer to the gel of tin cerium phosphate. Due to the redox activity of cerium present in the inorganic gel, aniline monomer was oxidized to polyaniline, and was formed in the interlayer of tin cerium phosphate. The resulting gel was kept for 24 hrs at room temperature maintaining the pH at 1. The pH was adjusted with 1.0 M NaOH/1.0 M $HNO_3$. It was then filtered, washed with deionized water, and dried. The exchanger was then converted into the $H^+$ form by treating it with 1.0 M $HNO_3$ for 24 hrs with occasional shaking and intermittent changing of acid. It was then washed with deionized water to remove the excess acid, dried, and sieved to obtain particles of 60-100 mesh.

*pH titrations:* The Topp and Pepper method

[29] was used for pH titrations using NaOH/ NaCl, KOH/KCl, systems, and 0.5 g of exchanger was equilibrated with varying amounts of metal chloride and metal hydroxide solutions. At equilibrium (after equilibration), the pH of the solutions was measured and plotted against the milliequivalents of $OH^-$ added.

*Ion-exchange capacity:* The ion exchange capacity of the material was determined by the column method. 1.0 g of the exchanger in $H^+$ form was taken in a glass column of 1.1 cm diameter. The $H^+$ ions were eluted by percolating 100 mL of 1.0 M NaCl solution. The effluent was collected and titrated against standard sodium hydroxide solution. The exchange capacity in $meqg^{-1}$ IEC was calculated using the formula

$$IEC = \frac{av}{w} \; IEC = \frac{av}{w}$$

where *a* is the molarity, *v* is the volume of alkali used during titration, and *w* is the weight of the exchanger taken [30].

*Effect of eluant concentration:* To find out the optimum concentration of the eluant for complete elution of $H^+$ ions, a fixed volume (100 ml) of NaCl solution of varying concentrations was passed through a column containing 1.0 g of the exchanger in the $H^+$ form with a flow rate of 0.5 ml $min^{-1}$. The effluent was titrated against a standard alkali solution of 0.1 M NaOH for the $H^+$ ions eluted out.

*Elution behavior:* Since an optimum concentration of 1.0 M NaCl for a complete elution of $H^+$ ions was observed for the sample, a column containing 1.0 g of the cation-exchanger in $H^+$ form was eluted with NaCl solution of this concentration in different 10 ml fractions with the minimum flow rate as described above. Each fraction of 10 ml effluent was titrated against a standard alkali solution for the $H^+$ ions eluted out.

*Thermal effect on ion-exchange capacity (I.E.C.):* To study the effect of drying temperature on the IEC, 1.0 g samples of the composite cation exchange materials in the $H^+$ form were heated at various temperatures in a muffle furnace for 2 hrs, and the $Na^+$ ion-exchange capacity was determined by the column process after cooling the materials at room temperature.

*Distribution coefficient ($K_d$):* Distribution studies were carried out for various metal ions in demineralized water by batch process. In this method, 0.1 g of the exchanger (60-100 mesh) was equilibrated with 20 mL of the metal ion solutions for 24 hrs at room temperature. The metal ion concentrations before and after sorption were determined by spectrophotometically/ complexometric titration against a standard EDTA solution. In the complexometric method, the $K_d$ values were calculated using the formula

$$K_d = \frac{(I-F)}{F} \times \frac{V}{W}$$

where I is the initial volume of EDTA used, F is the final volume of EDTA used, V is the volume of the metal ion solution (mL), and W is the weight of the exchanger [30].

*Adsorption Experiments:* Dye adsorption experiments were carried out using 10 mL stock solution of dye (10 $mgL^{-1}$). The dye was treated with a 0.2 g dose of the adsorbent. The variables studied were agitation time, adsorbent dose, and initial dye concentration. After the desired treatment time, the samples were filtered to remove the adsorbent. The progress of adsorption was estimated using a UV-visible spectrophotometer at 663 nm.

*Conductivity measurements:* The protonic conductivity of the materials was measured using pellets of 13 mm diameter and 1×5–2 mm thickness. The opposite sides of the pellets were coated with a conducting silver paste to ensure good electrical contact. Impedance measurements were taken using a 1255B FRA FI1287 electrochemical phase impedance analyser over a frequency range of 5 Hz to 1 MHz at a signal level below 1 V interfaced to a minicomputer for data collection. The measurements were made in the temperature range of 30–80 °C. In all cases, since the impedance plots of the material consisted of single depressed semi-circles, the pellet conductivity was calculated by arc extrapolation to the X-axis, taking into account the geometric size of the pellets.

*Antimicrobial activity:* The newly synthesized tin cerium phosphate-polyaniline was examined in antibacterial activities against *Staphylococcus aureus* bacterial strains. Petriplates containing 20ml Muller Hinton medium were seeded with 24 hrs culture of bacterial strain, *Staphylococcus aureus.* Wells of approximately 10mm were bored

using a well cutter and 25 µL, 50 µL and 100µL of sample was added to the well from a stock concentration of 0.1g/1mL. The plates were then incubated at 37 °C for 24 hrs. The antibacterial activity was assayed by measuring the diameter of the inhibition zone formed around the well (NCCLS, 1993). Gentamycin was used as a positive control.

## RESULTS AND DISCUSSION

The organic-inorganic nano composite tin cerium phosphate-polyaniline was prepared using a novel preparation strategy. The colour of the gel changed from yellow to green and finally to black by the addition of acidic aniline monomer solution into the tin cerium phosphate, which indicated the formation of polyaniline. The polyaniline formation in the matrix of inorganic exchanger is due to the redox action of cerium present in the tin cerium phosphate gel that oxidized the aniline and helped its polymerization. The earlier report of composite ion exchange material based on polyaniline showed that the preparation of composite material was done simply by adding the prepared gel of polyaniline into the inorganic matrix. The composite material obtained was black in colour.

In the FT-IR spectrum of the material (Fig. 1a), a strong broad band around 3400 $cm^{-1}$ was found which can be ascribed to the –OH stretching frequency. A sharp peak around 1600 $cm^{-1}$ can be attributed to the H–O–H bending band, which represents the strongly bonded –OH groups in the matrix. The –OH stretching bands merge together and shift to a lower frequency in the spectrum of the composite cation-exchanger. A strong broad band around 1000 $cm^{-1}$ may represent the presence of ionic phosphate groups. An assembly of two sharp peaks in the region of 500–800 $cm^{-1}$ may be due to the presence of a metal oxygen bond. These characteristic stretching frequencies showed a close resemblance with the inorganic precipitate tin cerium phosphate, indicating binding of the inorganic precipitate with the organic polymer and formation of an 'organic–inorganic' composite 'SnCeP-PANI'. Another assembly of two peaks in the region 1300–1400 $cm^{-1}$ of SnCeP-PANI may be ascribed to the stretching vibration frequency of C–N in the material [31], as it resembles the stretching vibration frequencies for C–N found in polyaniline. This proved that the SnCeP-PANI contains a considerable amount of polyaniline.

The XRD patterns of SnCeP (the reference) and SnCeP-PANI composites are shown in Fig. 1b. The X-ray diffraction pattern of the SnCeP showed no observable peaks that confirmed to the amorphous nature of the material. XRD analysis displayed the crystalline nature of the composite exchanger with a high intensity peak of 2θ value; the average crystalline size was found to be in the 30-40 nm range. The crystallinity of the composite material may be the result of the intercalation of polyaniline in between the SnCeP layer, which may be possible by the in-situ preparation strategy. The intercalation of polyaniline was proven with the support of the d value of the composite material [32]. The particle size was calculated from the full width at half-maximum of the peak using the Debye Scherrer equation

$$D = \frac{0.9\lambda}{\beta_{2\theta} \cos\theta_{max}}$$

where D is the average crystal size in nm, λ is the characteristic wavelength of the x-ray used, $\vartheta_{max}$ is the diffraction angle, and $\beta_{2\theta}$ is the angular width in radians at an intensity equal to

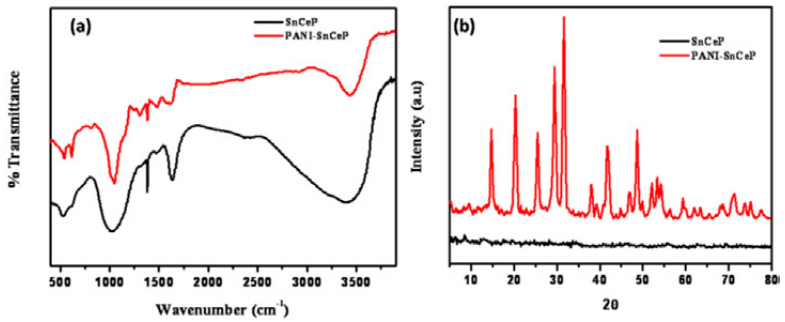


Fig. 1, a) FTIR spectra and b) XRD of SnCeP and SnCeP-PANI.

half of the maximum peak intensity. The results of XRD pattern indicate that nanocomposite is well crystalline and reveals all diffraction peaks, which are perfectly similar to the JCPDS data (Card No. 41–1445). The characteristic peaks appeared at 15°, 20.5°and 26°, corresponding to (011), (020) and (200) crystal planes of PANI. The XRD pattern of SnCeP-PANI shows that the (200) peak is the strongest, which indicates preferential growth in a certain direction. The peaks at 2θ values of 37.9° and 54.2° may be due to the (200) and (220) plane of crystalline $SnO_2$ present in the composite which shows the corresponding d (2.37 and 1.68 respectively) values of these planes. The peaks at 2θ values of 28.5°, 33.6°, 47°, and 58° may be due to (111), (200), (220) and (222) crystal plane of $CeO_2$ present in the composite matched with JCPDS File No. 34-0394.

Scanning electron microscope (SEM) photographs of SnCeP and SnCeP-PANI are shown in the Fig. 2a and Fig. 2b respectively. The SEM pictures demonstrate the difference in surface morphology of the inorganic exchanger and composite material. It has been revealed that after binding of polyaniline with SnCeP, the morphology has changed to a needle like structure, which may be due to the in-situ preparation strategy.

The TGA curve (Fig. 3a) of both samples recorded continuous weight loss of mass up to 150°C, which may be due to the removal of external water molecules [33]. For the composite material, there was a sudden weight loss at 550 °C, which may be due to the decomposition of the organic part. From 601°C onwards, a smooth horizontal section represents the complete formation of the oxide form of the material.

The pH titration curve obtained under equilibrium conditions for each of the NaOH/NaCl and KOH/KCl systems showed two inflection points, which indicate the bifunctional behavior of the material (Fig. 3b). It appears to be a strong cation exchanger as indicated by a low pH (~2.1) of the solution when no $OH^-$ ions were added to the system. The exchange capacity obtained from the

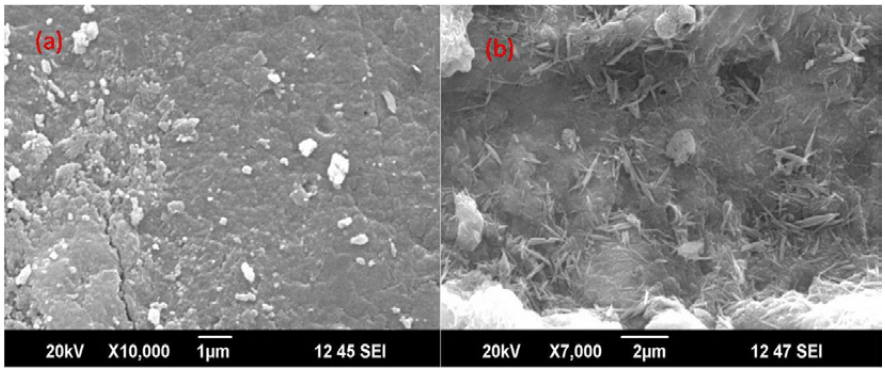


Fig. 2. SEM images of (a) SnCeP and (b) PANI-SnCeP.

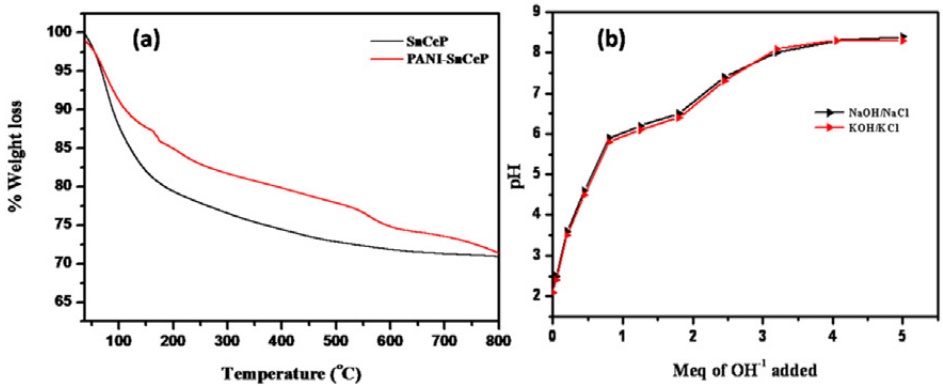


Fig. 3, a) TGA of SnCeP and SnCeP-PANI and b) pH titration curve of SnCeP-PANI.

Table 1. Effect of hydrated ionic radii and charge on IEC.

| Metal ion | Hydrated ionic radii (A°) | IEC ($meqg^{-1}$) |
|---|---|---|
| Li(I) | 3.40 | 1.34 |
| Na(I) | 2.76 | 1.28 |
| K(I) | 2.32 | 1.00 |
| Mg(II) | 7.00 | 0.98 |
| Ca(II) | 6.30 | 0.69 |
| Ba(II) | 5.90 | 0.47 |

Table 2. $K_d$ values of various metal ions in different electrolyte.

| Metal ions | DMW | 0.001 M $HNO_3$ | 0.01 M $HNO_3$ | 0.1 M $HNO_3$ | 0.001 M $NH_4NO_3$ | 0.01 M $NH_4NO_3$ | 0.1 M $NH_4NO_3$ |
|---|---|---|---|---|---|---|---|
| Pb(II) | 336.00 | 321.90 | 300.20 | 267.00 | 335.90 | 299.76 | 234.12 |
| Cu(II) | 139.60 | 130.90 | 122.00 | 87.90 | 130.90 | 96.10 | 56.00 |
| Zn(II) | 62.00 | 45.67 | 12.30 | 2.90 | 60.40 | 33.10 | 5.60 |
| Mg(II) | 25.40 | 12.00 | NA | NA | 25.00 | 10.90 | NA |
| Mn(II) | 73.40 | 70.12 | 34.22 | 10.10 | 70.46 | 23.50 | 7.80 |
| Bi(III) | 169.20 | 150.00 | 123.00 | 100.10 | 160.90 | 134.50 | 98.12 |
| Ca(II) | 18.95 | 8.99 | NA | NA | 17.89 | NA | NA |
| Hg(II) | 81.90 | 75.67 | 32.10 | 9.90 | 80.90 | 56.70 | 23.33 |
| Ni(II) | 39.80 | 29.00 | 11.11 | NA | 38.80 | 13.20 | NA |
| Co(II) | 66.00 | 62.11 | 31.11 | 16.70 | 60.70 | 21.90 | 9.90 |
| Cd(II) | 60.00 | 50.00 | 21.10 | 5.60 | 59.00 | 21.00 | 8.90 |

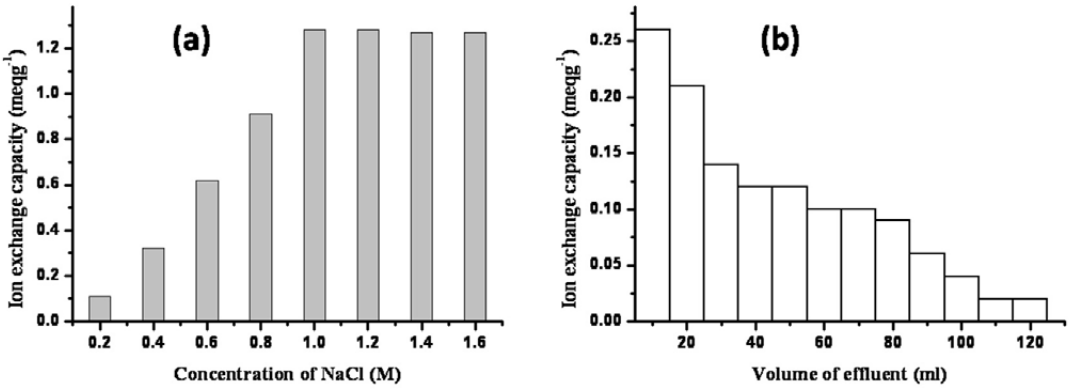


Fig. 4, a) Effect of eluent concentration on ion-exchange capacity, b) Elution behavior of SnCeP-PANI.

curve is in agreement with that obtained by the column method.

The composite material possessed an ion exchange capacity of 1.28 $meqg^{-1}$, which is higher than its inorganic counterpart tin cerium phosphate (0.92 $meqg^{-1}$). Improvement in ion exchange capacity of the composite material is considered to be due to the presence of a binding polymer (polyaniline). To check the reproducibility of the prepared composite, it was synthesized four times, under identical conditions of the concentration of reagents, the mixing ratio, and the drying temperature. The ion-exchange capacity and yield of each product were examined. The averages and standard deviations of the ion-exchange capacity and yield were found to be 1.28 $meqg^{-1}$ and ± 0.04%, respectively. Ion exchange capacities for mono (alkali) and bivalent (alkaline earth) metal ions were studied for determining the effects of the size and charge of the exchanging ion on the ion exchange capacity (Table 1). The ion-exchange capacity of the composite cation exchanger for alkali metal ions (except $Na^+$) and alkaline earth metal ions increased as their hydrated ionic radii decreased.

The column elution experiment indicated that the concentration of the eluent depended on the rate of elution, which is normal behavior for such

materials. A maximum elution was observed with a concentration of 1.0 M NaCl, as indicated in Fig. 4a. The elution behavior of the exchanger (Fig. 4b) reveals that the rate of exchange is quite fast as only 100 mL of NaCl solution (1.0 M) is needed for almost complete elution of $H^+$ ions from the column containing the 1.0 g exchanger. Hence, fast kinetics would facilitate the operation of the column for the separation of metal ions.

It was observed that on heating at different temperatures for 3 hrs, the mass and ion-exchange capacity of the exchanger changed as the temperature increased (Fig. 5). The composite cation exchange material was found to possess good thermal stability as the sample maintained about 60% of its initial mass by heating up to 400 °C. However, regarding ion exchange capacity, this material was found to possess better thermal stability than its counterparts as the sample maintained 70% of the ion-exchange capacity up to 150 °C, and it retained about 31% of the initial ion-exchange capacity when heated up to 300 °C and 11% up to 500 °C, whereas tin cerium phosphate retained only 8% of its ion exchange capacity when heated up to 500 °C.

The solubility experiment indicated that the composite material has reasonably good chemical stability as the results showed that the material was resistant to solutions of different acids, bases, organic solvents, and salts. The chemical stability may be due to the presence of a binding polymer that can prevent the dissolution or leaching of any constituent element into the solution.

To understand the potentiality of the composite cation-exchange material in the separation of metal ions, distribution studies for 11 metal ions were performed in various electrolytes (Table 2). The SnCeP-PANI composite ion exchange has a wide variety of $K_d$ values for different metal ions and has higher selectivity towards Pb(II) and Bi(III) in comparison to the other metal ions studied. The selectivity was found to be in the order of Pb(II) > Bi(III) > Cu(II) > Hg(II) > Mn(II) > Co(II) > Zn(II) > Cd(II) > Ni(II) > Mg(II) > Ca(II). The distribution studies proved that the selectivity of the composite toward the metal ions increased compared to the selectivity of its inorganic counterparts.

We studied the effect of polyaniline incorporation into the inorganic matrix of SnCeP on the dye adsorption to distinguish its potential use in the environmental applications. Adsorption of methylene blue (MB) on SnCeP and SnCeP-PANI dye using diffuse reflectance UV-visible spectroscopy was conducted for SnCeP and SnCeP-PANI, as is shown in Fig. 6. After treatment with materials for 2 hrs, the adsorption intensity of the MB solution decreased for the SnCeP-PANI treated MB solution compared to the adsorption intensity of the other. For the SnCeP treated MB solution, the adsorption maxima shifted from its original position, while for composite treated material MB solution, no shift was observed. The shift in the adsorption maxima indicated that the dye material changed from its original structure to another form. This suggested that for the SnCeP treated MB, degradation of dyes occurs, whereas for the SnCeP-PANI treated MB, adsorption rather than degradation happened. The 50 mg $g^{-1}$ solution of methylene blue was treated with SnCeP-PANI for 2 hrs with the percentage removal of dye found to be 99%, which is a comparatively high adsorption percentage when compared to other synthetic

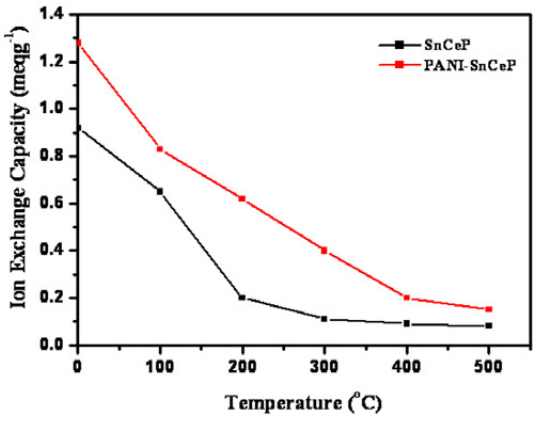


Fig. 5. Effect of temperature on IEC of SnCeP and SnCeP-PANI.

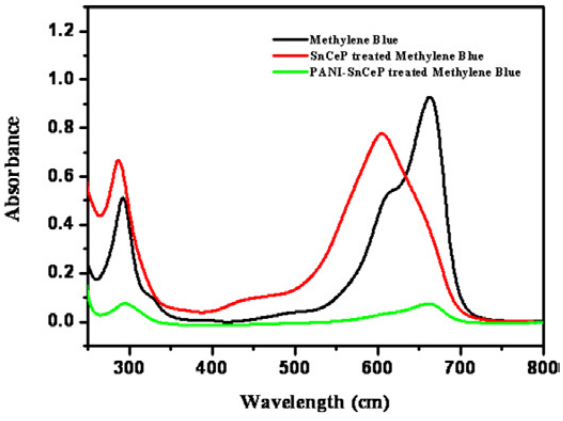


Fig. 6. Methylene blue adsorption on SnCeP and SnCeP-PANI.

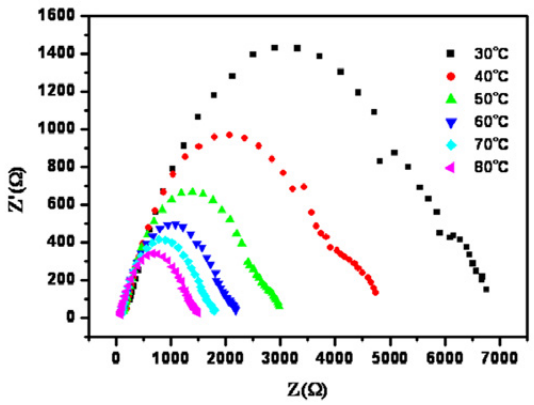


Fig. 7. Impedance spectra of SnCeP-PANI at different temperature range of 30-80°C.

composite materials.

The impedance plots for SnCeP-PANI at different temperatures are shown in Fig. 7. The impedance spectra consist of a single depressed semicircle. Sample resistance (R) was measured by extrapolation of the high frequency arc crossing the Z axis. Proton conductivity was measured using eq, σ = l/RA, where σ is conductivity, l is sample thickness, and A is electrode area ($cm^2$). Arrehinus plots (logσT vs 1/T) are shown for SnCeP and SnCeP-PANI in Fig. 8a and 8b, respectively. Activation energy for each sample was calculated using the Arrehius equation [$\sigma = \sigma_O \exp(-E_a/kT)$] where k is the Boltzman constant and T is the temperature.

Conductivity was measured in the range of 30–80°C for SnCeP and SnCeP-PANI. The conductivity data are presented in Table 3. As calculated from the electron impedance spectra, the sample SnCeP and SnCeP-PANI achieved a proton conductivity of $6.50\times10^{-4}$ and $3.61\times10^{-3}$ S $cm^{-1}$, respectively, at 90% relative humidity and 30°C. Arrhenius plots for the linearity of the two materials were observed in a temperature range of 30–80°C (Fig. 8). From specific conductance for SnCeP and SnCeP-PANI, it was observed that conductance increases with increasing temperature (Table 3). This fact is also supported by the study of heating effects on IEC, suggesting that the mechanism of transportation to be the Grotthus type, where conductivity depends on the ability of water located on the surface to rotate and participate [34]. Further results are also in agreement with the suggestion that the protons are not able to diffuse along an anhydrous surface where spacing of the –OH groups is too high [35]. Although all the conductivities shown here increase with increasing temperature, the absolute conductivity values clearly vary with each other. The proton migration is dominantly through the Grotthuss mechanism. In this mechanism, the

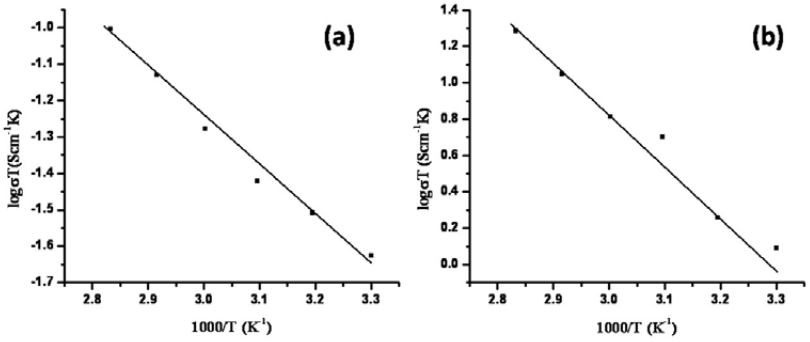


Fig. 8. Arrhenius plot for (a) SnCeP and (b) SnCeP-PANI in the temperature range of 30-80 °C.

Table 3. Specific conductance of SnCeP and SnCeP-PANI at various temperatures.

| Temperature (K) | Specific conductivity σ ($Scm^{-1}$) | |
|---|---|---|
| | SnCeP | SnCeP-PANI |
| 303 | $6.50\times10^{-4}$ | $3.61\times10^{-3}$ |
| 313 | $7.08\times10^{-4}$ | $4.14\times10^{-3}$ |
| 323 | $7.48\times10^{-4}$ | $6.24\times10^{-3}$ |
| 333 | $8.37\times10^{-4}$ | $6.77\times10^{-3}$ |
| 343 | $9.42\times10^{-4}$ | $8.32\times10^{-3}$ |
| 353 | $1.04\times10^{-3}$ | $1.02\times10^{-2}$ |
| Ea/$kcalmol^{-1}$ | 0.89 | 2.13 |

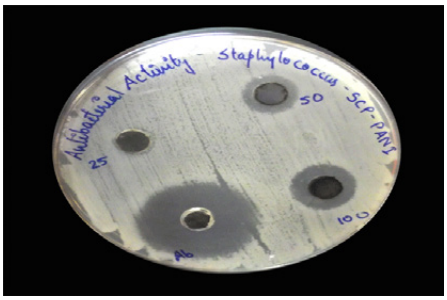


Fig. 9. Photographic images of zone of inhibition for *staphylococcus aureus* on SnCeP-PANI.

Table 4. Organism: *Staphylococcus aureus.*

| Sample | Volume of Sample (µL) | Zone of inhibition (mm) |
|---|---|---|
| Gentamycin | | 27 |
| **Sample –SnCeP-Pi** | | |
| | 25µL | Nil |
| | 50 µL | 14 |
| | 100 µL | 17 |

proton transport is mainly caused by the protons hopping from one water molecule to another through a tunnelling mechanism. To a smaller extent, the protons form a hydrogen bond with the water molecules and exit as $H_3O^+$, and diffusion of $H_3O^+$ ions enhances proton transport. The increase in temperature strongly affects both mechanisms; hopping as well as diffusion both becomes faster.

The higher conductivity value of SnCeP-PANI compared with that of SnCeP can be correlated with the IEC values of these materials. Higher IEC values indicate more exchangeable protons and hence more available conducting protons. They are in agreement with the pH value of the exchangers. $\sigma_{SnCeP\text{-}PANI}$ is higher compared to that of $\sigma_{SnCeP}$ due to the presence of the conducting polymer. However, observed conductance depends on the concentration of charge carriers, availability of vacant sites, crystal structure, surface morphology, and hydrophobicity, presence of interstitial sites, temperature, and activation energy [36].

The energy of activation (Ea, $kcalmol^{-1}$) values observed were 0.89 for SnCeP and 2.13 for SnCeP-PANI. The activation energy at saturated humidity was less, which means there is a lower energy barrier for the proton conduction [37]. Therefore, both observations indicate that water molecules adsorbed by the composite material promote proton conduction to a high degree. This is mainly due to the adsorbed water molecules that form the proton channels in the interlayers of the inorganic matrix for the smooth transfer of protons. Ea values follow the order SnCeP-PANI < SnCeP; however, σ values follow the order SnCeP < SnCeP-PANI. This shows no correlation with the order of conductivity of the exchanger presented. The materials SnCeP and SnCeP-PANI synthesized in our laboratory have higher specific proton conductance when compared to other materials discussed in previous studies.

SnCeP-PANI showed a promising antimicrobial activity at all concentrations (50, 100 µL) for inhibiting the growth of *Staphylococcus aureus* bacteria. The analysis data are described in the Table 4. Area of zone of inhibition is used as a criterion to ascertain the biocidal activity. According to this criterion, 10 mm to 17 mm zone of inhibition zone would represent significant activity. The photographic image of antibacterial study (*Staphylococcus aureus*) of SnCeP-PANI is shown in Fig. 9. The mechanism responsible for antimicrobial activity involves the rupturing of bacterial cell wall due to the binding of composite which release ions that react with the thiol groups (-SH) present on the bacterial cell surface to the outer membrane of *Staphylococcus aureus*. The heavy metal present in composite also inhibits the active transport and retards the enzyme activity, thus deactivating the proteins, rupturing the cell membrane and eventually causing the cell lysis [38, 39]. The presence of *staphylococcus aureus* was found in the wastewater plant. By using the tin cerium phosphate-polyaniline along with other ion exchangers used in the wastewater treatment

plant we can control the growth of the bacteria *staphylococcus aureus* in the wastewater plant.

## CONCLUSIONS

The highly crystalline nano composite tin cerium phosphate-polyaniline was prepared by a novel method. This nano composite exhibits good ion exchange capacity, thermal stability, and chemical resistivity, and it has a high ion exchange capability with lead metal ions. It showed good adsorptive power for the uptake of methylene blue dye from aqueous solution. The ion exchange and adsorption behavior of this composite are important from the viewpoint of environmental pollution chemistry, where an effective separation method is needed for the removal of heavy metal ions and dyes from aqueous systems. The materials presented in this paper also have higher proton conductivity compared to other materials already reported; hence, they will be promising candidates for use in the field of electrochemical devices. Composite material has an effective antimicrobial activity against *staphylococcus aureus* bacteria. In view of all these outcomes, it may be concluded that SnCeP-PANI composite ion exchanger could be a potential candidate for the environmental remediation.

## ACKNOWLEDGEMENTS

The authors gratefully acknowledge STIC, Cochin, Biogenix, Trivandrum for instrumental support.

## CONFLICT OF INTERESTS

There is no conflict of interest.

## REFERENCES

[1] Sharma G., Pathania D., Naushad M., Kothiyal N. C., (2014), Fabrication, characterization and antimicrobial activity of polyaniline Th(IV) tungstomolybdophosphate nanocomposite material: Efficient removal of toxic metal ions from water. *Chem. Eng. J.* 251: 413–421.

[2] Gupta V. K., Pathania D., Asif M., Sharma G., (2014), Liquid phase synthesis of pectin–cadmium sulfide nanocomposite and its photocatalytic and antibacterial activity. *J. Mol. Liq.* 196: 107–112.

[3] Wanhong S., Wenbo Zh., Hailing Li., Qiong Su., Ping Zh., Lihua Ch., (2020), Insight into the synergistic effect on adsorption for Cr (VI) by a polypyrrole-based composite. *RSC Adv.* 10: 8790-8799.

[4] Oneeb U. H., Jae-Hwan Ch., Youn-Sik L., (2020), Synthesis of ion-exchange polypyrrole/activated carbon composites and their characterization as electrodes for capacitive deionization. *Macromolecule. Res.* 28: 877–880.

[5] Daniel A. A., Vairathevar S. V., (2020), Hollow polypyrrole composite synthesis for detection of trace-level toxic herbicide. *ACS Omega*. 5: 21458-21467.

[6] Judeinstein P., S´anchez C., (1996), Hybrid organic-inorganic materials: A land of multidisciplinarity. *J. Mater. Chem.* 6: 511–525.

[7] Ruiz-Hitzky E., Casal B., Aranda P., Galv´an J. C., (2001), Inorganic-organic nanocomposite materials based on macrocyclic compounds. *Rev. Inorg. Chem.* 21: 125–159.

[8] Meneghetti P., Qutubuddin S., (2004), Synthesis of poly(methyl methacrylate) nanocomposites via emulsion polymerization using a zwitterionic surfactant. *Langm.* 20: 3424–3430.

[9] Qiang X., Chunfang Z., Zun Y. J., Yuan C. S., (2004), The effects of polymer-nanofiller interactions on the dynamical mechanical properties of PMMA/$CaCO_3$ composites prepared by microemulsion template. *J. Appl. Polym. Sci.* 91: 2739-2749.

[10] Chujo Y., (1996), Organic—inorganic hybrid materials. *Curr. Opin. Solid. State. Mater. Sci.* 1: 806-811.

[11] Sanchez C., Ribot F., (1994), Design of hybrid organic-inorganic materials synthesized via sol–gel chemistry. *New. J. Chem.* 16: 1007-1047.

[12] Judeinstein P., Sanchez C., (1996), Hybrid organic–inorganic materials: A land of multidisciplinarity. *J. Mater. Chem.* 6: 511-517.

[13] Mark J. E., Lee C. Y., Bianconi P. A., (1995), Eds hybrid organic–inorganic composites. *Am. Chem. Soc.*, Washington.

[14] Douglas J. C., Douglas H., Pamela J. Z., Robert P. H., Robert L., Robert C. H., Zubieta J., (1999), Organic/inorganic composite materials: The roles of organoamine ligands in the design of inorganic solids. *Coord. Chem. Rev.* 737: 190–192.

[15] Pathania D., Sharma G., Naushad M., Kumar A., (2014), Synthesis and characterization of a new nanocomposite cation exchanger polyacrylamide Ce (IV) silicophosphate: Photocatalytic and antimicrobial applications. *J. Ind. Eng. Chem.* 20: 3596–3603.

[16] Pathania D., Sharma G., Kothiyal N. C., Kumar A., (2014), Fabrication of nanocomposite polyaniline zirconium(IV) silicophosphate for photocatalytic and antimicrobial activity. *J. Alloys. Compd.* 588: 668–675.

[17] ALOthman Z. A., Naushad M., (2011), Adsorption thermodynamics of trichloroacetic acid herbicide on polypyrrole Th(IV) phosphate composite cation-exchanger. *Chem. Eng. J.* 169: 38–42.

[18] Gupta V. K., Pathania D., Kothiyal N. C., Sharma G., (2014), Polyaniline zirconium (IV) silicophosphate nanocomposite for remediation of methylene blue dye from waste water. *J. Mol. Liquid.* 190: 139–145.

[19] Khan A. A., Paquiza L., (2011), Characterization and ion-exchange behavior of thermally stable nano-composite polyaniline zirconium titanium phosphate: its analytical application in separation of toxic metals. *Desalination.* 265: 242–254.

[20] Nabi S. A., Bushra R., Naushad M., Khan A., (2010), Synthesis, characterization and analytical applications of a new composite cation exchange material, poly-o-toluidine stannicmolybdate for the separation of toxic metal ions. *Chem. Eng. J.* 165: 529–536.

[21] AL-Othman Z. A., Naushad M., (2011), Organic–inorganic type composite cation exchanger poly-o-toluidine Zr(IV) tungstate: Preparation, physicochemical characterization and its analytical application in separation of heavy metals.

*Chem. Eng. J.* 172: 369–375.
[22] Jacinth M. K., Regini C., Subramaniam P., Murugesan R., (2020), Poly(O-Toluidine)/Zirconium-based nanocomposite ion-exchangers for water treatment and environmental remediation. *J. Water Environ. Nanotechnol.* 5: 17-33.
[23] Shirakawa H., Louis E., Macdiarmid A. G., Chiang C. K., Hegger A. J., (1977), Synthesis of electrically conducting organic polymers: Halogen derivatives of polyacetylene (CH)x. *J. Chem. Soc. Chem. Commun.* 16: 578–580.
[24] Zafar Alam I., Nabi S. A., (2010), Synthesis and characterization of a thermally stable strongly acidic Cd (II) ion selective composite cation-exchanger: Polyaniline Ce(IV) molybdate. *Desalination.* 250: 515-522.
[25] Khan A. A., (2006), Preparation, physicochemical characterization, analytical applications and electrical conductivity measurement studies of an 'organic-inorganic' composite cation-exchanger: Polyaniline Sn(IV) phosphate. *React. Funct. Polym.* 66: 1649-1663.
[26] Debashish A., Bidhan M., Piyush P., Malabika S., Farnaj N., (2017), Optical and antibacterial properties of synthesised silver nanoparticles. *Micro Nano Lett.* 12: 223–226.
[27] Pathania D., Sharma G., Naushad M., Kumar A., (2014), Synthesis and characterization of a new nanocomposite cation exchanger polyacrylamide Ce (IV) silicophosphate: Photocatalytic and antimicrobial applications. *J. Ind. Eng. Chem.* 20: 3596–3603.
[28] Nabi S. A., Shahadat M., Bushra R., Oves M., Ahmed F., (2011), Synthesis and characterization of polyaniline Zr(IV) sulphosalicylate composite and its applications electrical conductivity and antimicrobial activity studies. *Chem. Eng. J.* 173: 706–714.
[29] Topp N. E., Pepper K. W., (1949), Properties of ion-exchange resins in relation to their structure. Part I. Titration curves. *J. Chem. Soc.* 3299-3303.
[30] Vogel A. I., (1975), A text book of quantitative inorganic analysis, Longman Group Limited, London.
[31] Duval C., (1963), Inorganic Thermogravimetric Analysis, *Elsevier,* Amsterdam, pp315.
[32] Rao CNR., (1963), Chemical Applications of Infrared Spectroscopy, *Academic Press*, New York.
[33] Celly M. S. I., Vera R. L. C., Marcia. L. A. T., (2008), Polyaniline/layered zirconium phosphate nanocomposites: Secondary-like doped polyaniline obtained by the layer-by-layer technique. *J. Nanosci. Nanotechnol.* 8: 1782-1789.
[34] Clearfield A., (1988), Role of ion exchange in solid-state chemistry. *J. Mol. Catal.* 88: 125-132.
[35] Alberti G., Costantino U., Polambari R., (1989), First international conference on inorganic membranes, Montpellier, France, 25.
[36] Padmakumar P., Yashonath S., (2006), Ionic conduction in the solid state. *J. Chem. Sci.* 118: 135-154.
[37] Chandra S., Singh N., Hashmi S. A., (1986), Proton conduction insolids. *Proc. Ind. Nat. Sci. Acad.* 52A: 338-343.
[38] Cook G., Costerton J. W., Darouiche R. O., (2000), Direct confocal microscopy studies of the bacterial colonization in vitro of a silver-coated heart valve sewing cuff. *Int. J. Anti. Agent.* 13: 169-173.
[39] Jennifer A., Ayandiran A., Oluwafayoke O., Deborah O., Folashade A., Olusola M., Adaramola F. B., (2021), Biogenic synthesis and characterization of Silver nanoparticles from seed extract of *Spondia mombins* and screening of its antibacterial activity. *Int. J. Nano. Dimens.* 12: 175-185.